Superhydrophobic Surfaces

International Edition: DOI: 10.1002/anie.201411023
German Edition: DOI: 10.1002/ange.201411023

Direct Insight into the Three-Dimensional Internal Morphology of Solid–Liquid–Vapor Interfaces at Microscale**

Shuai Yang, Jiexing Du, Moyuan Cao, Xi Yao, Jie Ju, Xu Jin, Bin Su, Kesong Liu, and Lei Jiang*

Abstract: *Solid–liquid–vapor interfaces dominated by the three-phase contact line, usually performing as the active center in reactions, are important in biological and industrial processes. In this contribution, we provide direct three-dimensional (3D) experimental evidence for the inside morphology of interfaces with either Cassie or Wenzel states at micron level using X-ray micro-computed tomography, which allows us to accurately "see inside" the morphological structures and quantitatively visualize their internal 3D fine structures and phases in intact samples. Furthermore, the in-depth measurements revealed that the liquid randomly and partly located on the top of protrusions on the natural and artificial superhydrophobic surfaces in Cassie regime, resulting from thermodynamically optimal minimization of the surface energy. These new findings are useful for the optimization of classical wetting theories and models, which should promote the surface scientific and technological developments.*

Since the famous Young's equation was proposed in 1805, many different theoretical models (such as Wenzel and Cassie states and transition between the Cassie and Wenzel states) have been proposed to explain wetting behaviors on solid surfaces,[1–6] which remarkably promoted the development in surface and interface sciences.[7–13] However, there are still some theoretical disputes for predicting wetting behavior in different circumstances, arising from the lack of a direct insight into solid–liquid–vapor interfaces.[14] Moreover, the detection of internal solid–liquid–vapor interfaces dominated by the three-phase contact line (TCL) is of relevance for fundamental investigations and practical applications in, for example, coatings, paints, medical science, biotechnology, electronics, aerospace, lubrication, textiles, paper, and cosmetic industries.[15–20] Therefore, the in situ, direct, and in-depth insight of the inside solid–liquid–vapor TCL morphology, especially three-dimensional (3D) geometry at microscale, is crucial to the further enrichment and improvement of fundamental wetting theories as well as the rational design of functional surfaces with special wettability.[21–24]

During the past few years, a variety of experimental strategies including atomic force microscopy,[25] confocal laser scanning microscope,[26] cryogenic focused ion-beam scanning electron microscopy,[27] and environmental scanning electron microscopy,[28] have been applied to investigate the TCL morphology on solid surfaces. However, these approaches are limited to scan small part of the whole contact morphology, which hardly demonstrate the entire and internal TCL morphological structures. These technical limitations impeded to further observe the inner interface morphology. Therefore, using the conventional surface analysis techniques, it is still a challenge to obtain the internal information of the solid–liquid–vapor TCL without any destruction.

Herein we reveal the three-dimensional (3D) internal morphology of solid–liquid–vapor micro-interfaces with Cassie and Wenzel states on either natural or artificial surfaces by using in situ high-resolution X-ray micro-computed tomography (Micro-CT). Furthermore, the direct and quantitative observations of the inside trapped air cushion between droplets and solid surfaces are also achieved for the first time. Noteworthy, the in-depth experimental insights unveil that the air pockets exist in the inner interface and liquid partly contacts the protrusions. This is distinct from the classical Cassie theory, which predicts that liquids contact each protrusion and the inner contact line is flat. These new findings provide more elaborate and precise information for the internal TCL morphology, which will contribute to the improvement of wetting theories and models as well as to surface scientific development.

Micro-CT is an in situ, nondestructive 3D imaging system suited for structural analysis of a variety of samples including, for example, semiconductors, geological materials, and biological materials.[29] In this contribution, Micro-CT was first developed to quantitatively investigate the internal morphology of solid–liquid–vapor micro-interfaces, which allows us to analyze and visualize its fine 3D internal structures in intact

[*] Dr. S. Yang, J. Du, Dr. M. Cao, Dr. X. Jin, Prof. K. Liu, Prof. L. Jiang
Key Laboratory of Bio-inspired Smart Interfacial Science and Technology of Ministry of Education
School of Chemistry and Environment, Beihang University
Beijing 100191 (P.R. China)
E-mail: liuks@buaa.edu.cn
Dr. X. Yao, Dr. J. Ju, Prof. B. Su, Prof. L. Jiang
Beijing National Laboratory for Molecular Sciences
Key Laboratory of Organic Solids
Institute of Chemistry Chinese Academy of Science
Beijing 100190 (P. R. China)
Dr. X. Jin
Research Institute of Petroleum, Exploration and Development, PetroChina, Beijing (P. R. China)

[**] We appreciate the financial support of National Natural Science Foundation (grant numbers 21273016, 21421061, 91127025, and 21431009), Australian Research Council (grant number DP140102581), Program for New Century Excellent Talents in University, Beijing Natural Science Foundation (grant number 2122035), National Research Fund for Fundamental Key Projects (grant number 2013CB933000), Beijing Higher Education Young Elite Teacher Project, the Key Research Program of the Chinese Academy of Sciences (grant number KJZD-EW-M01), the 111 project (grant number B14009), and the Fundamental Research Funds for the Central Universities.

Supporting information for this article is available on the WWW under http://dx.doi.org/10.1002/anie.201411023.

samples. This is challengeable for the conventional surface analysis technique. Micro-CT uses the attenuation of X-rays by various units spaced within angular intervals to create the 3D and 2D high-resolution images (see the Supporting Information note S1). During the process, virtual slices of solid–liquid–vapor interfaces at microscale can be acquired noninvasively at various planes (Figure 1).

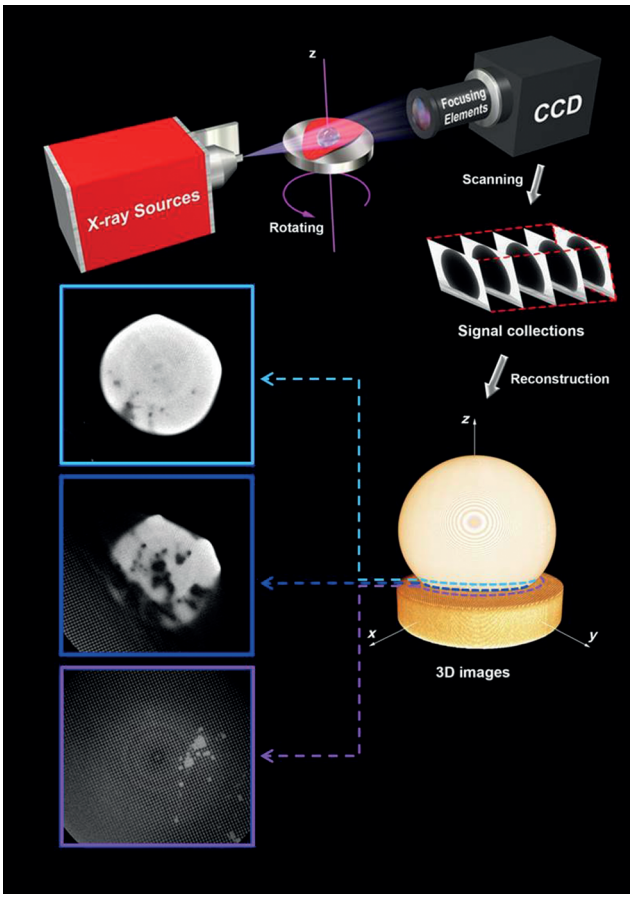

Figure 1. The schematic principle and measurement of Micro-CT. An individual Micro-CT slice can be extracted from the reconstructed 3D copy of the sample to obtain detailed information. The extracted slices from top to bottom in the *x*–*y* plane clearly show the inner morphology of the solid–liquid–vapor micro-interface. Bright, dark, and gray represent liquid, vapor, and solid phases, respectively.

The conventional theoretical model proposed that the wetting regime of the lotus leaf is in the Cassie state, where the droplet contacts with the top of each papilla and the air pocket is flat.[30–32] However, the acquisition of the internal TCL experimental evidence is still a challenge to verify this hypothesis. Here, the individual Micro-CT slice clearly revealed the existence of an air cushion between the lotus leaf and the droplet (Figure 2A). The magnified image (Figure 2B) demonstrated that the droplet partly contacts with the top of papillae, resulting in the internal discontinuous air pockets at microscale. This can be further confirmed by the reconstructed Micro-CT stack presented in movie S1 in the Supporting Information. The curved solid–liquid–vapor interface was also observed on the artificial superhydrophobic

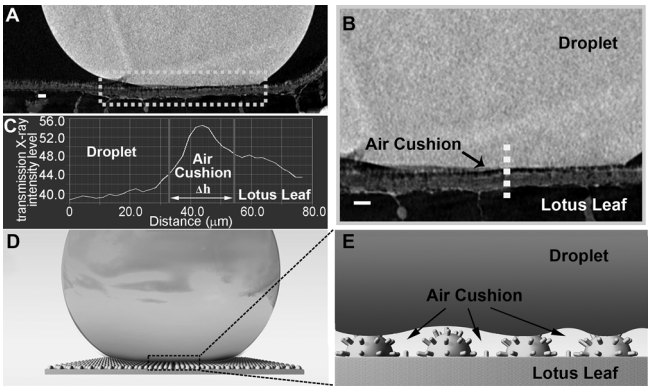

Figure 2. Micro-CT results and schematic illustrations of the internal solid–liquid–vapor TCL morphology on the superhydrophobic lotus leaf. A) An individual Micro-CT slice demonstrated the existence of air cushion in the interface (scale bar 50 μm). B) The enlarged Micro-CT slice showed that the liquid partly located on the top of papillae, resulting in a dome interface and a discontinuous air pocket (scale bar 50 μm). C) Owing to the absorption and phase contrast, Micro-CT could quantitatively calculate the thickness of the air pocket (along the yellow dotted line in Figure 2B). The thickness of the air pocket is 18.7 ± 1.9 μm. D,E) Schematic of the internal contact state of the liquid on the lotus leaf based on the Micro-CT experimental results.

surface discussed in the following section. Figures 2D and E schematized the contact state on lotus leaves at different magnifications on the basis of the Micro-CT internal observation. The observations of the air pockets of the inner interface under the liquid are distinctly different from the classical Cassie description, where the liquid locates on the top of each asperity and the inner contact line is flat. Arising from the absorption, Micro-CT could accurately investigate the TCL and quantitatively calculate the thickness of the air cushion. As shown in Figure 2C, the X-ray transmission intensity of the air cushion is much higher than that of the liquid and the lotus leaf. The thickness of the air pocket is 18.7 ± 1.9 μm.

For the superhydrophobic red rose petal, the internal TCL information is still a mystery.[33,34] The results exhibited that the liquid directly contacts with micropapillae at microscale (Figure 3A and see movie S2). The magnified image (Figure 3B) further demonstrated that the internal micropapillae arrays have been infiltrated without the existence of an air pocket. The schematic representation of the contact state for the liquid on the red rose petal were presented in Figure 3D and E, exhibiting the classical Wenzel regime at microscale. No X-ray transmission intensity-induced peak was observed in Figure 3c, indicating the full infiltration of petal surfaces and the absence of the air cushion.

In order to further investigate the internal TCL structures, representative superhydrophobic surfaces with Cassie and Wenzel regimes were also fabricated on the silicon substrate with patterned micropillar arrays. For the superhydrophobic surface with the Cassie state, the individual Micro-CT tomographic slice shown in Figure 4A indicated that the liquid does not infiltrate into the space between the silicon pillars. The magnified image clearly demonstrated the existence of an air cushion at the micron scale between the liquid and the

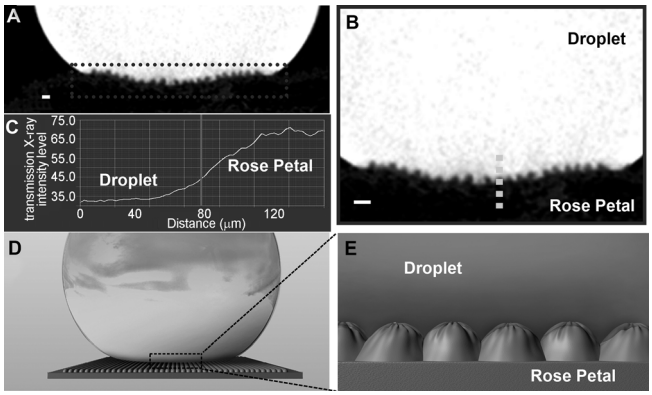

Figure 3. Micro-CT experimental results and schematic representation of the internal TCL morphology on the superhydrophobic red rose petal. A) The individual Micro-CT slice showed that the liquid directly contacts with micropapillae on the petal surface at microscale (scale bar 50 μm). B) The high-magnification slice indicated that the liquid fully infiltrated into the micropapillae (scale bar 50 μm). C) No X-ray transmission intensity-induced peak was detected (along the yellow dotted line in Figure 3 B), indicating the full infiltration of petal surfaces. D,E) Schematic of the internal contact state of the liquid on the red rose petal.

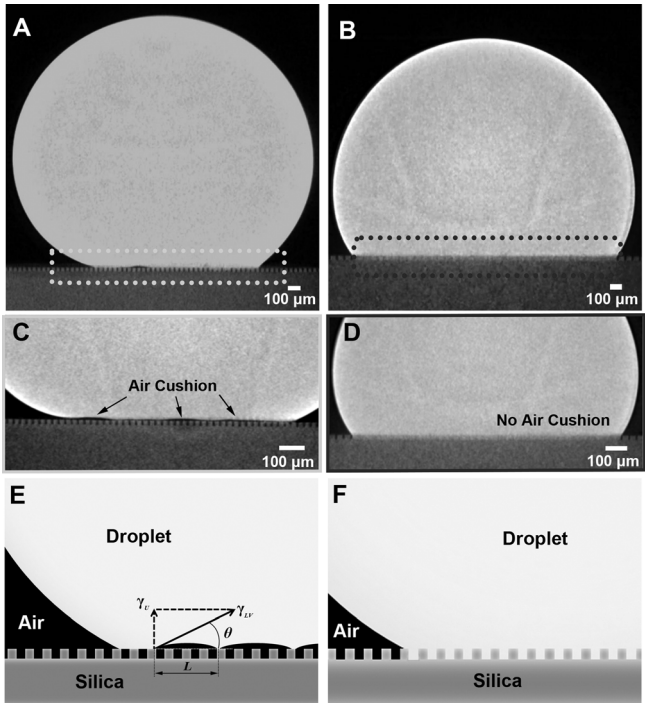

Figure 4. Typical internal solid-liquid–vapor interfaces of the liquid on artificial superhydrophobic surfaces with Cassie or Wenzel states. A) Micro-CT slice of the Cassie state surface indicated that the liquid does not fill in silicon pillar grooves. B,D) Micro-CT slices of the Wenzel state surface at different magnification exhibited that the silicon pillar grooves were entirely infiltrated. C) The enlarged slice of the Cassie state surface demonstrated the presence of an air cushion at microscale. E) The mechanism and function of dome interface on the superhydrophobic Cassie-state surface. F) Schematic of the internal contact state of the liquid on the Wenzel surface, showing the absence of an air cushion under the liquid.

silicon surface (Figure 4 C). Furthermore, it was found that the liquid randomly and partly contacted with the top of silicon pillars, resulting in the discontinuous air pockets, which is consistent with the above experimental study conducted on the natural lotus leaf (see note S2). This is distinct from the classical description in the Cassie model, where the liquid fully contacts with the top of each protrusions and the air cushion is flat. This novel observation can be further confirmed by the reconstructed Micro-CT stacks in both horizontal and longitudinal cross-sections, which allow us to "see inside" the solid–liquid–vapor TCL and visualize its internal morphology at microscale (see movies S3 and S4). For the superhydrophobic surface with the Wenzel state, both the Micro-CT slices and the reconstructed stacks showed that the liquid was fully infiltrated into the pillars grooves and no air cushion existed between the liquid and the silicon surface (Figure 4 B and D, see movies S5 and S6).

Force analysis of air pockets indicates that two opposite surface tensions are combined to balance the dome shapes at microscale (see note S3). Investigations of the system surface energy of the system show that the presence of air pockets is thermodynamically favored and contributes to the robust superhydrophobicity[35] (see note S4). This is an important advance in the direct clarification of the robust superhydrophobic mechanism. This result is consistent with the findings of Pokroy and co-workers, which showed small curvature of the liquid interface in the whole droplet.[36] The visualized observation of the inside morphology can also be used to clarify some wetting phenomena, including calculations of the contact angle,[37] intrinsic mechanism for the low adhesion, and the small sliding angle of the liquid on superhydrophobic Cassie surfaces (see note S5).

In summary, Micro-CT was first developed to quantitatively and accurately investigated the inside morphology of the solid–liquid–vapor TCL with either Cassie or Wenzel states at microscale, which allowed us to "see inside" the morphological structures and visualize their internal 3D fine structures. Key fundamental questions of solid–liquid–vapor TCL in surface science, including, for example, the internal morphology, structure, and phases have been solved by this approach, which is a challenge for the conventional analysis techniques. The in-depth insights of the interface at microscale in the Cassie regime, different from the classical Cassie description, facilitate the accurate measurements of the contact angle and the direct clarification of robust superhydrophobicity, low adhesion, small low sliding angle, and other wetting-related phenomena. All these new findings will be immensely beneficial for the further optimization and improvement of theoretical wetting models as well as the promotion of surface scientific and technological developments.

Keywords: Cassie and Wenzel states · micro-computed tomography · superhydrophobicity · surface science · wettability

How to cite: *Angew. Chem. Int. Ed.* **2015**, *54*, 4792–4795
Angew. Chem. **2015**, *127*, 4874–4877

[1] L. Feng, S. H. Li, Y. S. Li, H. J. Li, L. J. Zhang, J. Zhai, Y. L. Song, B. Q. Liu, L. Jiang, D. B. Zhu, *Adv. Mater.* **2002**, *14*, 1857 – 1860.
[2] A. Lafuma, D. Quéré, *Nat. Mater.* **2003**, *2*, 457 – 460.
[3] X. J. Feng, L. Jiang, *Adv. Mater.* **2006**, *18*, 3063 – 3078.
[4] T. Young, *Philos. Trans. R. Soc. London* **1805**, *95*, 65 – 87.
[5] R. N. Wenzel, *Ind. Eng. Chem.* **1936**, *28*, 988 – 994.
[6] A. B. D. Cassie, S. Baxter, *Trans. Faraday Soc.* **1944**, *40*, 546 – 551.
[7] K. Liu, X. Yao, L. Jiang, *Chem. Soc. Rev.* **2010**, *39*, 3240 – 3255.
[8] D. Quéré, *Annu. Rev. Mater. Res.* **2008**, *38*, 71 – 99.
[9] M. Prakash, D. Quéré, J. W. M. Bush, *Science* **2008**, *320*, 931 – 934.
[10] A. Tuteja, W. Choi, M. Ma, J. M. Mabry, S. A. Mazzella, G. C. Rutledge, G. H. McKinley, R. E. Cohen, *Science* **2007**, *318*, 1618 – 1622.
[11] K. Liu, L. Jiang, *Annu. Rev. Mater. Res.* **2012**, *42*, 231 – 263.
[12] M. W. Denny, *Science* **2008**, *320*, 886.
[13] B. Pokroy, A. K. Epstein, M. C. M. Persson-Gulda, J. Aizenberg, *Adv. Mater.* **2009**, *21*, 463 – 469.
[14] P. Ball, *Nat. Mater.* **2009**, *8*, 250 – 250.
[15] T. S. Wong, S. H. Kang, S. K. Y. Tang, E. J. Smythe, B. D. Hatton, A. Grinthal, J. Aizenberg, *Nature* **2011**, *477*, 443 – 447.
[16] K. S. Liu, Y. Tian, L. Jiang, *Prog. Mater. Sci.* **2013**, *58*, 503 – 564.
[17] H. Bellanger, T. Darmanin, E. T. de Givenchy, F. Guittard, *Chem. Rev.* **2014**, *114*, 2694 – 2716.
[18] K. Li, J. Ju, Z. X. Xue, J. Ma, L. Feng, S. Gao, L. Jiang, *Nat. Commun.* **2013**, *4*, 2276.
[19] K. Liu, L. Jiang, *Nano Today* **2011**, *6*, 155 – 175.
[20] J. Genzer, A. Marmur, *MRS Bull.* **2008**, *33*, 742 – 746.
[21] X. F. Gao, L. Jiang, *Nature* **2004**, *432*, 36 – 36.
[22] Y. M. Zheng, H. Bai, Z. B. Huang, X. L. Tian, F. Q. Nie, Y. Zhao, J. Zhai, L. Jiang, *Nature* **2010**, *463*, 640 – 643.
[23] J. C. Contreras-Naranjo, V. M. Ugaz, *Nat. Commun.* **2013**, *4*, 1919.
[24] J. Ju, H. Bai, Y. M. Zheng, T. Y. Zhao, R. C. Fang, L. Jiang, *Nat. Commun.* **2012**, *3*, 1247.
[25] P. Chen, L. Chen, D. Han, J. Zhai, Y. Zheng, L. Jiang, *Small* **2009**, *5*, 908 – 912.
[26] C. Luo, H. Zheng, L. Wang, H. Fang, J. Hu, C. Fan, Y. Cao, J. Wang, *Angew. Chem. Int. Ed.* **2010**, *49*, 9145 – 9148; *Angew. Chem.* **2010**, *122*, 9331 – 9334.
[27] K. Rykaczewski, T. Landin, M. L. Walker, J. H. J. Scott, K. K. Varanasi, *ACS Nano* **2012**, *6*, 9326 – 9334.
[28] A. T. Paxson, K. K. Varanasi, *Nat. Commun.* **2013**, *4*, 1492.
[29] A. Sakdinawat, D. Attwood, *Nat. Photonics* **2010**, *4*, 840 – 848.
[30] W. Barthlott, C. Neinhuis, *Planta* **1997**, *202*, 1 – 8.
[31] C. Neinhuis, W. Barthlott, *Ann. Bot.* **1997**, *79*, 667 – 677.
[32] B. Bhushan, Y. C. Jung, *Prog. Mater. Sci.* **2011**, *56*, 1 – 108.
[33] L. Feng, Y. A. Zhang, J. M. Xi, Y. Zhu, N. Wang, F. Xia, L. Jiang, *Langmuir* **2008**, *24*, 4114 – 4119.
[34] B. Bhushan, E. K. Her, *Langmuir* **2010**, *26*, 8207 – 8217.
[35] A. Marmur, *Langmuir* **2003**, *19*, 8343 – 8348.
[36] B. Haimov, S. Pechook, O. Ternyak, B. Pokroy, *J. Phys. Chem. C* **2013**, *117*, 6658 – 6663.
[37] A. Marmur, *Soft Matter* **2006**, *2*, 12 – 17.

Received: November 23, 2014
Published online: February 12, 2015

